

From quantum matter to high-temperature superconductivity in copper oxides

B. Keimer¹, S. A. Kivelson², M. R. Norman³, S. Uchida⁴ & J. Zaanen⁵

The discovery of high-temperature superconductivity in the copper oxides in 1986 triggered a huge amount of innovative scientific inquiry. In the almost three decades since, much has been learned about the novel forms of quantum matter that are exhibited in these strongly correlated electron systems. A qualitative understanding of the nature of the superconducting state itself has been achieved. However, unresolved issues include the astonishing complexity of the phase diagram, the unprecedented prominence of various forms of collective fluctuations, and the simplicity and insensitivity to material details of the ‘normal’ state at elevated temperatures.

The discovery of high-temperature superconductivity in the copper oxide perovskite $\text{La}_{2-x}\text{Ba}_x\text{CuO}_4$ (ref. 1) ranks among the major scientific events of the twentieth century. The superconducting transition temperatures in the copper oxides greatly exceed those of any previously known superconductor by almost an order of magnitude; in 1986 the highest possible temperature at which superconductivity could survive was widely believed to be 30 K (Fig. 1). Moreover, according to the theory of ‘conventional’ superconductors, the copper oxides would have seemed the least likely materials in which to look for superconductivity: at room temperature they are such poor conductors that they can hardly be classified as metals and, indeed, if their chemical composition is very slightly altered they become highly insulating antiferromagnets. Magnetism arises from strong repulsive interactions between electrons, whereas conventional superconductivity arises from induced attractive interactions, making magnetism and superconductivity seemingly anti-thetical forms of order.

The Bardeen–Cooper–Schrieffer (BCS) theory² of the late 1950s provided an extremely successful framework within which to understand conventional superconductors, and gave rise to conceptual breakthroughs. The basic insight is that the electrons collectively bind into ‘Cooper’ pairs and simultaneously condense in much the same way as bosons condense into a superfluid state. Fundamental to the BCS mechanism is the fact that, despite the strong direct Coulomb repulsions, the relatively weak attractions between electrons induced by the coupling to the vibrations of the lattice (phonons) can bind the electrons into pairs at energies smaller than the typical phonon energy. This was widely believed to imply that the superconducting transition temperature T_c of conventional superconductors could never exceed 30 K (ref. 3), although this limit has been revised upwards by the discovery in 2001 of superconductivity with $T_c = 39$ K in the simple metal MgB_2 (ref. 4), where circumstances conspire to optimize the electron–phonon mechanism. However, this is still far below the maximum T_c of the copper oxides.

As the properties of the copper oxides were studied with ever-increasing precision and sensitivity, it became clear that much of the well-understood quantum theory of the electronic properties of solids, which has been spectacularly successful in accounting for the properties of conventional metals and superconductors, fails entirely to address many features of the copper oxides and, more generally, of a broad array of ‘highly correlated electron systems’ of which the copper oxides are the most studied. (A schematic phase diagram of the copper oxides is shown in Fig. 2.)

Most prominently, at temperatures well above T_c the conductivity in the copper oxides is almost two orders of magnitude smaller than in simple metals and exhibits frequency and temperature dependences that are incompatible with the conventional theory of metals; this has led to materials in the regime above T_c being referred to as ‘strange metals’ or ‘bad metals’. The behaviour exhibited by these ‘strange metals’, much of which is simple to describe in terms of the so-called “marginal-Fermi-liquid phenomenology”⁵, has resisted any generally accepted understanding. On the other hand, similar behaviour has now been documented in a large number of electronically interesting materials⁶, indicating that this is a general property of strongly correlated electron systems, and is not directly linked to high-temperature superconductivity. We consider this to

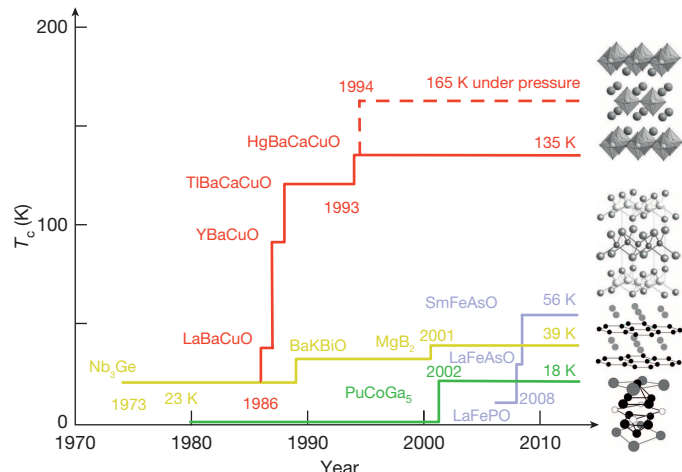


Figure 1 | T_c versus time. Superconducting transition temperatures versus year of discovery for various classes of superconductors. The images on the right are the crystal structures of representative materials. The established record for conventional electron–phonon superconductors (yellow) is 39 K in MgB_2 . Given the small Fermi energies, the T_c values found in the family of heavy fermion superconductors (green) are actually remarkably high. There has been much interest in recent years in the new family of ‘iron superconductors’ (purple) in which T_c values approach 60 K. The record holders are found in the copper oxide family (red), with a maximum T_c of 165 K found in a ‘mercury’ copper oxide under pressure (dashed red line).

¹Max Planck Institute for Solid State Research, Heisenbergstrasse 1, D-70569 Stuttgart, Germany. ²Department of Physics, Stanford University, Stanford, California 94305, USA. ³Materials Science Division, Argonne National Laboratory, Argonne, Illinois 60439, USA. ⁴Department of Physics, University of Tokyo, Bunkyo-ku, Tokyo 113-0033, Japan. ⁵Lorentz Institute for Theoretical Physics, Universiteit Leiden, PO Box 9506, 2300 RA Leiden, The Netherlands.

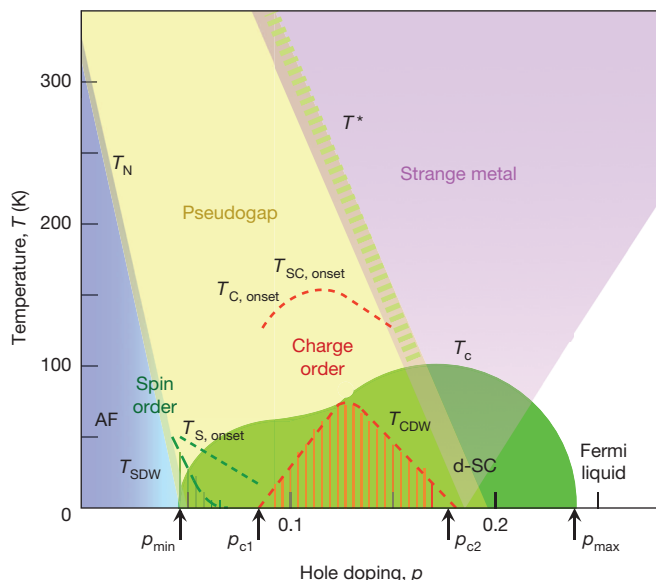


Figure 2 | Phase diagram. Temperature versus hole doping level for the copper oxides, indicating where various phases occur. The subscript ‘onset’ marks the temperature at which the precursor order or fluctuations become apparent. $T_{S,\text{onset}}$ (dotted green line), $T_{C,\text{onset}}$ and $T_{SC,\text{onset}}$ (dotted red line for both) refer to the onset temperatures of spin-, charge and superconducting fluctuations, while T^* indicates the temperature where the crossover to the pseudogap regime occurs. The blue and green regions indicate fully developed antiferromagnetic order (AF) and *d*-wave superconducting order (d-SC) setting in at the Néel and superconducting transition temperatures T_N and T_c , respectively. The red striped area indicates the presence of fully developed charge order setting in at T_{CDW} . T_{SDW} represents the same for incommensurate spin density wave order. Quantum critical points for superconductivity and charge order are indicated by the arrows.

be the most important open problem in the understanding of quantum materials, and it is here that radically new ideas, including those derived from recently developed non-perturbative studies in string theory, may be useful.

More unique to the copper oxides is the behaviour observed in a range of temperatures immediately above T_c in what is referred to as the ‘pseudogap’ regime. It is characterized by a substantial suppression of the electronic density of states at low energies that cannot be simply related to the occurrence of any form of broken symmetry. Although much about this regime is still unclear, convincing experimental evidence has recently emerged that there are strong and ubiquitous tendencies towards several sorts of order or incipient order, including various forms of charge-density-wave, spin-density-wave, and electron-nematic order. There is also suggestive, but far from definitive, evidence of several sorts of novel order—that is, never before documented patterns of broken symmetry—including orbital loop current order and a spatially modulated superconducting phase referred to as a ‘pair-density wave’. There are many fascinating aspects of these ‘intertwined orders’ that remain to be understood, but their existence and many aspects of their general structure were anticipated by theory⁷. Superconducting fluctuations also have an important role in part of this regime, although to an extent that is still much debated.

The high-temperature superconducting phase itself has a pattern of broken symmetry that is distinct from that of conventional superconductors. Unlike in conventional *s*-wave superconductors, the superconducting wavefunction in the copper oxides has *d*-wave symmetry^{8,9}, that is, it changes sign upon rotation by 90°. Associated with this ‘unconventional pairing’ is the existence of zero energy (gapless) quasiparticle excitations at the lowest temperatures, which make even the thermodynamic properties entirely distinct from those of conventional superconductors (which are fully gapped). The reasons for this, and its relation to a proximate anti-ferromagnetic phase, are now well understood, and indeed were also anticipated early on by some theories^{10–12}. However, while various attempts

to obtain a semiquantitative estimate of T_c have had some success¹³, there are important reasons to consider this problem still substantially unsolved.

Highly correlated electrons in the copper oxides

The chemistry of the copper oxides amplifies the Coulomb repulsions between electrons. The two-dimensional copper oxide layers (Fig. 3) are separated by ionic, electronically inert, buffer layers. The stoichiometric ‘parent’ compound (Fig. 2, zero doping) has an odd-integer number of electrons per CuO₂ unit cell (Fig. 3). The states formed in the CuO₂ unit cells are sufficiently well localized that, as would be the case in a collection of well-separated atoms, it takes a large energy (the Hubbard U) to remove an electron from one site and add it to another. This effect produces a ‘traffic jam’ of electrons¹⁴. An insulator produced by this classical jamming effect is referred to as a “Mott insulator”¹⁵. However, even a localized electron has a spin whose orientation remains a dynamical degree of freedom. Virtual hopping of these electrons produces, via the Pauli exclusion principle, an antiferromagnetic interaction between neighbouring spins. This, in turn, leads to a simple (Néel) ordered phase below room temperature, in which there are static magnetic moments on the Cu sites with a direction that reverses from one Cu to the next^{16,17}.

The Cu-O planes are ‘doped’ by changing the chemical makeup of interleaved ‘charge-reservoir’ layers so that electrons are removed (hole-doped) or added (electron-doped) to the copper oxide planes (see the horizontal axis of Fig. 2). In the interest of brevity, we will confine our discussion to hole-doped systems. Hole doping rapidly suppresses the antiferromagnetic order. At a critical doping of p_{\min} , superconductivity sets in, with a transition temperature that grows to a maximum at p_{opt} then declines for higher dopings and vanishes for p_{\max} (Fig. 2). Materials with $p < p_{\text{opt}}$ are referred to as underdoped and those with $p_{\text{opt}} < p$ are referred to as overdoped.

It is important to recognize that the strong electron repulsions that cause the undoped system to be an insulator (with an energy gap of 2 eV) are still the dominant microscopic interactions, even in optimally doped copper oxide superconductors. This has several general consequences. The resulting electron fluid is ‘highly correlated’, in the sense that for an electron to move through the crystal, other electrons must shift to get out of its way. In contrast, in the Fermi liquid description of simple metals, the quasiparticles (which can be thought of as ‘dressed’ electrons) propagate freely through an effective medium defined by the rest of the electrons. The failure of the quasiparticle paradigm is most acute in the ‘strange metal’ regime, that is, the ‘normal’ state out of which the pseudogap and the superconducting phases emerge when the temperature is lowered. Nonetheless, in some cases, despite the strong correlations, an emergent Fermi liquid arises at low temperatures. This is especially clear in the overdoped regime (Fig. 2). But recently it has been shown that even in underdoped materials, at temperatures low enough to quench superconductivity by the application of a high magnetic field, emergent Fermi liquid behaviour

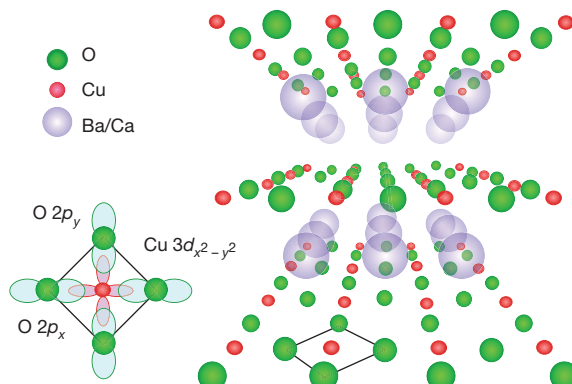


Figure 3 | Crystal structure. Layered copper oxides are composed of CuO₂ planes, typically separated by insulating spacer layers. The electronic structure of these planes primarily involves hybridization of a $3d_{x^2-y^2}$ hole on the copper sites with planar-coordinated $2p_x$ and $2p_y$ oxygen orbitals.

arises, albeit with characteristics (for example, a reconstructed Fermi surface) that are quite different from those predicted by band theory^{18,19}. Nevertheless, over most of the phase diagram, the frustration of the coherent electron motion produces physics that is qualitatively distinct from that of simple metals.

Although the large zero-point energy of electrons in a usual metal results in a quantum ‘rigidity’ that greatly suppresses all forms of inhomogeneous states, the Mott physics and the short-range antiferromagnetic correlations inherited from the undoped ‘parent’ compound combine to produce a local tendency to phase separation and various forms of order, which spontaneously break the translational symmetry of the underlying crystal^{20–22}. Thus, especially in the pseudogap regime of the phase diagram, it is unsurprising that various forms of order occur on intermediate length scales.

Pairing in an unconventional superconductor

It is now well established that electrons can form pairs, even when they repel each other at a microscopic scale. However, this involves non-trivial physics. A model that is often used as a point of departure for theoretical discussions is the famous Hubbard model, describing electrons hopping on a lattice parametrized in terms of the bandwidth $W = 8t$ (where t is a measure of the ‘hopping’ energy gain due to delocalization of the electrons) and an on-site electron-electron repulsion U . In the copper oxides, U and W are comparable. Even for this simplified model, analytic solutions are not available. However, approximate solutions of the doped Hubbard model can be obtained in several ways, and these invariably point to a d -wave superconducting ground state.

An intuitive understanding of the mechanism of pairing is best obtained by approaching the problem from an unrealistic weak-coupling perspective, that is, assuming $U \ll W$ (ref. 23). Here, the gap structure is determined by the solution of a variant of the original BCS equations, in which an appropriately renormalized two-particle vertex function, $\Gamma(\mathbf{k})$, plays the part of an effective interaction. For the case of purely repulsive interactions, if Γ is sufficiently \mathbf{k} -dependent, a sign-changing superconducting order parameter (where $\Delta(\mathbf{k})$ and $\Delta(\mathbf{k} + \mathbf{Q})$ have opposite sign) results for which interactions involving small momentum transfer are pair-breaking, and those with large momentum transfer near \mathbf{Q} promote pairing. In particular, if there are antiferromagnetic correlations, this typically implies a peak in Γ at the antiferromagnetic ordering vector, $\mathbf{Q} = \mathbf{Q}_{\text{AF}}$ (ref. 24), which is also an ideal vector for scattering between ‘antinodal’ regions of the Fermi surface of the copper oxides shown in Fig. 4; that is, precisely those regions where the d -wave gap is largest and of opposite sign. The gap ‘nodes’ along the diagonals of the Brillouin zone are then, in turn, where the d -wave gap vanishes.

Superconductivity in the Hubbard model cannot truly be approached from the strong-coupling limit, since there is now strong numerical evidence that for a broad range of doping, the ground state of the Hubbard model is ferromagnetic rather than superconducting for large enough U/t (ref. 25). However, the closely related t - J model (with $J = 4t^2/U$ being the superexchange interaction between copper spins mediated by the intervening oxygen ions) incorporates the essence of the strong-coupling physics through the constraint that no more than one electron at a time can occupy a given site. The t - J model can then be addressed, with values of $J/t \approx 0.5$, as a reasonable model in its own right. Although no controlled solution is known, the superconducting tendencies of this model have been investigated numerically since the early days of high-temperature superconductivity research^{26,27}. It is striking that the character and symmetry of the superconducting state itself and its association with short-range antiferromagnetic correlations look grossly similar, regardless of perspective²⁴.

Although intermediate coupling problems have thus far not been successfully solved by controlled analytic approaches, the lack of any small dimensionless parameters probably implies the lack of any long emergent length scales in the problem, except near a quantum critical point (QCP). With this in mind, a variety of numerical techniques have been developed to study this regime, including exact diagonalization (limited to small clusters), quantum Monte Carlo and its derivatives (variational

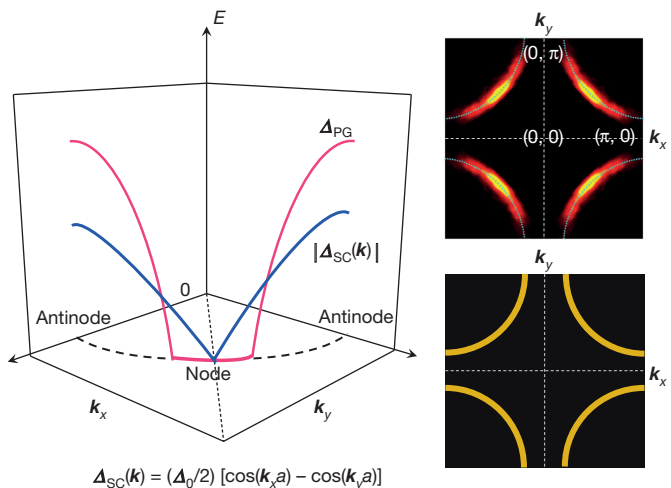


Figure 4 | Fermi surface, Fermi arcs and gap functions. The large Fermi surface predicted by band theory is observed by ARPES and STS for overdoped compounds (bottom right). But once the pseudogap sets in, the antinodal regions of the Fermi surface near the Brillouin zone edge are gapped out, giving rise to Fermi arcs (top right). This is reflected (left) in the angle dependence of the energy E of the superconducting gap Δ_{SC} (blue line) and pseudogap Δ_{PG} (red line) as functions of the momenta k_x and k_y in one quadrant of the Brillouin zone around the underlying large Fermi surface (dashed curve), as revealed by ARPES and STS. Note the gapless region around the d -wave superconducting node for the pseudogap case that defines the Fermi arcs. These arcs appear to be reconstructed into electron pockets centred at $(Q/2, Q/2)$ once charge order sets in, as revealed by quantum oscillation studies, where $(Q, 0)$ is the charge order wavevector¹⁹.

and fixed node approximations to get around the issue of negative probabilities in fermion simulations), dynamical mean field theory²⁸ and its cluster generalizations (either in momentum space or real space), density matrix renormalization group (designed for one-dimensional problems but can simulate strips), and its two-dimensional generalizations²⁹. These methods all have their pros and cons. They have, however, taught us that if superconductivity occurs, it is invariably of d -wave symmetry, but also that many competing states are close in energy, especially unidirectional charge order^{30,31}.

High- T_c superconductivity

Of course, there is additional complexity in going from theoretical results for simple model problems to the real experimental systems. Static antiferromagnetism disappears quickly as a function of doping (Fig. 2), but both inelastic neutron scattering and resonant inelastic X-ray scattering reveal that the antiferromagnetism of the insulator survives in the superconductor to a degree in the form of dynamical magnetic fluctuations which are much stronger than in conventional metals (and are strongly renormalized when cooling below T_c)^{32–35}. It is physically appealing to use the measured spin fluctuation spectrum as an approximation of the vertex Γ mentioned above. This yields reasonable values for T_c , and also appears to be consistent with some of the single electron self-energy effects detected by various electron spectroscopies such as ARPES (angle resolved photo-emission spectroscopy) and STS (scanning tunnelling spectroscopy)^{13,36}.

However, this approach, departing from the idea of the attractive force (‘glue’) induced by spin fluctuations, has shortcomings³⁷. Despite its intuitive appeal, it is not based on controlled mathematics, since the same electrons that are pairing also form the ‘glue’. Another difficulty is that these simplified models leave out other effects that can influence the magnitude of T_c . A case in point is the electron–phonon interaction. There is good evidence that phonons affect both ARPES and STS line shapes³⁸, while strong anomalies are seen in the phonon spectra³⁹. There are a number of other neglected effects that are worrisome, in particular the non-local Coulomb interaction which is an especially relevant concern given the poor screening in the direction perpendicular to the planes⁴⁰.

More seriously, some fundamental aspects of high- T_c superconductivity are qualitatively different from the BCS variety. An example is the influence of quenched disorder. In absolute terms, most copper oxides can be regarded as chemically ‘dirty’, owing to their doped (non-stoichiometric) nature. In BCS theory, an important difference between *s*-wave and unconventional superconductivity is that the former is relatively impervious to structural disorder, while the latter is readily degraded⁴¹. The strong inhomogeneity seen by STS leaves no doubt that many copper oxide superconductors reside in a disordered lattice potential, but the *d*-wave superconductivity appears to be fairly insensitive to this adverse condition. It has been suggested that this is a consequence of strong local correlations⁴², but it still remains a puzzle.

A very basic quantity for the superconducting order is the superfluid density ρ_s , the quantity that parametrizes the rigidity of the phase of the superconducting order parameter, which also determines the capacity of the superconductor to expel electromagnetic fields. One can identify a temperature associated with the fluctuations of the phase $T_0 \approx \rho_s/m^*$ where m^* is the effective mass. In a BCS superconductor, ρ_s is equal to the total density of electrons at zero temperature and accordingly $T_0 \gg T_c \approx 0.5\Delta_0/k_B$, the temperature associated with the formation of the pairs where Δ_0 is the average superconducting gap (k_B is the Boltzmann constant). The fluctuations of the phase of the superconducting condensate are largely irrelevant; once Cooper pairs form, they automatically condense. Turning to the copper oxides, it was established early on that the superfluid density is anomalously small, scaling in the underdoped regime with T_c (the “Uemura law”⁴³). The conclusion is that in the underdoped copper oxides, T_0 and the pair-binding energy are of the same order and the thermal fluctuations of the phase should be crucial for the thermodynamics⁴⁴. A long-standing question is whether, perhaps, pairs already form at the (very high) pseudogap temperature T^* (Fig. 2), while at a much lower temperature, the actual T_c , the phase locks to form the long-range ordered superconducting state. As we will see, the physics of the phase fluctuations is intertwined with that of competing order.

In many cases, in copper oxides with the highest T_c (that is, at optimal doping), the superconductivity emerges directly as an instability of the strange metal phase. The strange metal is the least understood part of the phase diagram, because it does not appear to be describable in terms of weakly interacting Landau quasiparticles. The very non-BCS transition from the strange metal to the more conventional physics of the superconducting state is vividly apparent in the temperature evolution of the ARPES spectra at momenta near the ‘antinodes’ (Fig. 4) where the pairing forces of the *d*-wave superconductor are supposedly the strongest. For these momenta, the electron spectral function is strongly broadened as a function of energy⁴⁵. Upon entering the superconducting phase, a quasiparticle peak starts to develop that has the classic backbending (Bogoliubov) dispersion of a BCS superconductor⁴⁶. This is, in turn, consistent with the onset of coherence observed in microwave, infrared and thermal conductivities. But, unlike in BCS theory, it appears that the spectral weight of this antinodal ‘Bogoliubon’ is linearly proportional to the superfluid density, both as a function of doping and temperature^{47,48}. This is not understood: it is as if the phase coherence of the superconductor ‘freezes out’ single-particle coherence from the highly collective non-Fermi-liquid strange metal state.

Pseudogap regime

A prominent feature of this regime of the phase diagram is the line T^* , which denotes the onset of a partial gap observed in spectroscopic data. First inferred from nuclear magnetic resonance measurements that showed a reduction in the low-frequency spin excitations^{49,50}, this pseudogap was subsequently seen in *c*-axis polarized infrared conductivity measurements and is associated with a pronounced upturn in the *c*-axis resistivity⁵¹. In contrast, the in-plane polarized infrared conductivity indicates a drop in the scattering rate⁵², which is reflected in a reduction of the planar resistivity^{53,54}.

A much debated question is whether conventional (Hartree–Fock) mean-field treatments are able to provide even a qualitatively correct account of

the pseudogap phenomenology. There are surely issues related to the ‘plethora of orders’ discussed immediately below, something which is not easy to understand in the conventional way. However, one obtains a much sharper view using electron spectroscopies. The striking difference in the nature of the electronic excitations measured in ARPES when crossing from the ‘coherent’ nodal region to the ‘incoherent’ antinodal region in momentum space is called the nodal–antinodal dichotomy⁵⁵. The nodal region involves a narrow region around the zone diagonals, which gradually grows with increasing doping until it encompasses the entire Fermi surface in sufficiently overdoped materials. While the antinodal region lacks any quasiparticle-like spectral peaks, throughout the pseudogap regime it exhibits a suppression of low-energy electronic spectral weight on an energy scale that corresponds to the pseudogap⁴⁵.

The astonishing character of these observations is best illustrated by showing a map of the spectral weight at low energy as a function of \mathbf{k} in the first Brillouin zone (Fig. 4). In a Fermi liquid, the Fermi surface delineates the boundary between occupied and unoccupied quasiparticle states, so no matter how complicated it may be, the one thing it cannot do is abruptly end. However, in the pseudogap regime, there appear to be ‘Fermi arcs’ in the nodal regime⁵⁶. In a mean-field theory, the effective potential associated with a (density-wave) state that breaks translational symmetry can reconstruct a large Fermi surface, producing small Fermi surface pockets, but these must still form connected manifolds. It is plausible that the Fermi arcs are actually the front half of such a pocket^{57,58}, and hence there has been an intense search to find the ‘backside of the pocket’, but at present there is no definitive sign of it.

STS has proved particularly revealing in this context. Such data (mostly below T_c) exhibit electronic waves in real space that upon Fourier transformation show peaks that disperse with bias and have been mapped to scattering across the Fermi surface⁵⁹. One finds that in the superconducting state, the low-energy excitations near the nodes behave just as one would expect for a BCS *d*-wave state⁶⁰, but at higher energies, cross over to a dispersionless pattern characteristic of short-range stripe order. Interestingly, this low-energy dispersing pattern maps out the same Fermi arc⁶¹ in momentum space (Fig. 4) as observed directly by ARPES⁶² in the pseudogap state, with the arc recovering the full Fermi surface once the doping exceeds a critical value⁶². However, the STS result, indicating a complete loss of coherence in the antinodal regime, appears to be inconsistent with the ARPES, which sees antinodal quasiparticles below T_c , even for underdoped materials⁶³. The higher-energy dispersionless pattern is seen at all energies when moving above T_c into the pseudogap state^{64,65}, consistent with local charge order, and has been identified as coexisting with the low-energy dispersing signal below T_c as well^{66,67}. But the consistency of the ARPES data with charge order is still an active area of debate⁶⁸—to date, no unambiguous signatures associated with the stripe wavevectors have been found.

Precursor pairing

The structure of the pseudogap in momentum space was directly mapped by ARPES experiments at temperatures between T^* and T_c , and found to crudely mimic the *d*-wave superconducting gap: the pseudogap is apparent only in the ‘antinodal’ regions of the Brillouin zone (Fig. 4)^{57,69,70} where the *d*-wave gap is largest. This immediately suggests that at the very high pseudogap temperature T^* , pairs already start to form, while phase fluctuations prohibit superconducting order until much lower temperatures are reached. So long as there is substantial short-range phase coherence, superconducting fluctuations should have large and identifiable signatures. For instance, for a range of temperatures that extends up to about $1.5T_c$ (but not to temperatures comparable to T^*), large fluctuation conductivity (at both direct and alternating current) is observed⁷¹, but there is some debate about how much such signatures differ from those observed in classic superconductors.

The more far-reaching notion of pairing correlations without substantial phase coherence persisting to temperatures of the order of T^* is difficult to define precisely, even in principle. The best circumstantial evidence comes from diamagnetism, which is observed up to about 150 K (ref. 72).

Though weak compared to full Meissner screening, it is still large compared to that of simple metals. Moreover, in underdoped $\text{YBa}_2\text{Cu}_3\text{O}_{6+x}$ (YBCO), a moderately well-defined interlayer Josephson plasma resonance seems to persist up to similar temperatures⁷³, and recent pump–probe experiments are consistent with transient superconducting order existing all the way to T^* (ref. 74). Perhaps the most compelling evidence is in the temperature evolution of the gap itself; the nodal–antinodal dichotomy notwithstanding, the pseudogap above T_c evolves remarkably smoothly into the gap of the superconducting state well below T_c . In that context, it has been suggested by ARPES that the Fermi arc is simply due to the lifetime broadening of a d -wave node^{75,76}, and this has been inferred as well by STS below T_c (ref. 77). The reconciliation of this superconducting-like signature in the fermion response in the pseudogap phase and an energy gap due to competing order⁷⁸ has been a major challenge, even more relevant now, given the new findings of such crystalline order (see below).

Competing orders

Another increasingly well-documented feature of the pseudogap regime is a tendency towards a variety of orders (that is, patterns of broken symmetry) in addition to superconductivity. Some involve ‘crystallization’ of the electrons in the form of stripes and other forms of charge order, but others appear to be more novel quantum liquids. There is also some evidence for new types of order involving various patterns of equilibrium orbital currents, and possibly a new sort of spatially modulated superconducting state.

Neutron scattering studies in the mid-1990s led to the experimental discovery of electronic ‘stripes’ in the $\text{La}_{2-x}\text{Sr}_x\text{CuO}_4$ (LSCO) family²². These studies were inspired, in part, by earlier mean-field theories of density-wave formation in lightly doped Hubbard-like models²⁰. An alternative and complementary theoretical perspective was based on the observation that doping an insulating antiferromagnet produces a tendency to phase separation that is frustrated by the long-range Coulomb interaction; the compromise is to form conducting stripe-like textures²¹. The stripe order, characterized by incommensurate antiferromagnetic order and charge segregation, was initially found in underdoped versions of LSCO, where a low-temperature tetragonal lattice deformation apparently acts as a pinning potential for the stripes²². However, it became clear that these stripes were different from the ‘classical’ stripes in the other doped Mott insulators: the copper oxide stripes stay metallic and even superconduct at low temperatures. Although the spatial organization looks similar to the mean field stripes, a crucial difference is that these can now be viewed as a partially crystallized superconductor, formed from electron pairs^{31,79}.

In general terms, a competition between superconductivity and crystallization is a very natural way to account for the diminishing superfluid density in the pseudogap regime. Indeed, quite recently, evidence has emerged that materials with static stripes form a “pair density wave”: the charge stripes are internally superconducting, but the phase reverses from stripe to stripe⁷. Given that the stripe orientation changes as one moves from one layer to the next, this frustrates the Josephson coupling between layers, entirely extinguishing the superfluid stiffness perpendicular to the planes and thus giving rise to a two-dimensional superconducting state consistent with transport measurements^{80,81}. If confirmed, this would constitute the discovery of a new phase of matter.

It was subsequently found, by inelastic neutron scattering, that the magnetic spectrum of the ordered stripes has a unique ‘hourglass’ pattern⁸², with the neck of the hourglass located at the commensurate antiferromagnetic wavevector, and this pattern has subsequently been observed in the insulating charge ordered states of manganites and cobaltates⁸³. Although this makes it natural to associate the inelastic neutron scattering spectrum with the spin waves associated with incommensurate magnetic order, in the copper oxides, this pattern persists for larger dopings, even where the stripe order is no longer condensed and where the character of the spin-wave spectrum changes dramatically when the temperature drops below T_c (ref. 84). In this regime, many salient features of the magnetic spectrum are similar to what is expected for weakly interacting quasiparticles

in a homogeneous d -wave superconductor⁸⁵. A reconciliation of these two very different pictures remains a challenge for the field.

For many years, static stripe order had seemed to be confined to the LSCO family. However, recently charge ordering was discovered in underdoped YBCO⁸⁶ and Bi- and Hg-based copper oxides^{67,68,87}. X-ray experiments find short-range incommensurate charge order that gradually sets in between 100 K and 200 K (refs 88 and 89). Moreover, high-resolution X-ray scattering⁹⁰ and nuclear magnetic resonance experiments have confirmed that the short-range charge order is truly static, and thus presumably arises from pinning of correlated charge fluctuations by defects⁹¹. Unlike in the stripes of the LSCO family, there is no evidence of coincident static (or nearly static) magnetic order. Moreover, the variation of the stripe wavevector with doping in YBCO⁹² and Bi-based copper oxides^{67,68} is much weaker and has the opposite sign of that in LSCO. Whereas in LSCO, this wavevector increases with doping as would be expected in a real space picture, in YBCO and the Bi-based copper oxides, the wavevector decreases, as would be expected from a momentum space picture involving vectors spanning the Fermi surface. This difference may be connected with differences in the spin behaviour: in YBCO a large spin gap is present that acts to suppress the incommensurate spin order that is more prevalent in the LSCO family^{34,35}.

Yet another interesting hint regarding the unusual relationship between the charge order and superconductivity follows from the temperature evolution of the charge order. The X-ray signal begins to build up smoothly upon cooling below a characteristic charge ordering temperature (T_{CDW}) typically less than T^* , to attain a maximum at the superconducting T_c , then drops noticeably below T_c , indicating competition between the charge order and superconductivity^{88,89,92}.

There is also evidence for ‘quantum nematic liquid crystal’ order occurring in the pseudogap phase. Such phases are translationally invariant but break point group (for example, rotational) symmetries. First suggested in the context of the quantum melting of stripe crystals⁹³, evidence appeared for a phase breaking the fourfold symmetry of the square lattice in underdoped YBCO, from transport^{94,95} and inelastic neutron scattering measurements⁹⁶. This ‘nematic’ signal was also found in an analysis of the STS data, showing that besides the ‘stripy’ texture breaking translations, there is also an overall (zero wavevector) breaking of rotations present, consistent with the two oxygen ions in the CuO_2 unit becoming inequivalent^{97,98}, though this is controversial⁹⁹.

These orders are all close siblings of the electron crystal. However, there is also evidence for a completely different kind of order below T^* as well. This order is symmetry-wise equivalent to having magnetic moments on the oxygen sites, and thus would be a magnetic analogue of the charge nematic mentioned above¹⁰⁰. But the original proposal that motivated the experiments involved spontaneous electron currents flowing inside the CuO_2 units in such a way that although rotational symmetry is broken, translational symmetry is not¹⁰¹. It has a quite distinct magnetic diffraction pattern, which was subsequently seen by spin-flip neutron scattering¹⁰⁰. If confirmed, this would again amount to the discovery of a new phase of matter, though it does not yield a natural explanation for the pseudogap, just by the very fact that it does not break translational symmetry. The real difficulty with this proposal is that current order should also be seen by local magnetic probes such as muon spin resonance and nuclear magnetic resonance, but this has not been observed. Potentially related to this is the onset of a small Kerr rotation at T^* , which also indicates some type of symmetry breaking¹⁰². This Kerr signal defines a phase line that cuts through the superconducting dome, vanishing near 18% doping.

The strange metal

The strange metal regime was recognized early on as perhaps the most mysterious aspect of the copper oxide phase diagram. The most basic difference between the strange metal and a conventional metal is the absence of quasiparticles. This has consequences for physical properties like the electrical resistivity. In a normal metal, unless the metal melts first, the resistivity saturates at high temperatures when the mean free path, l , becomes

of the order of the electron de Broglie wavelength, λ . The resistivity of the copper oxide strange metal can be linear in T from near T_c up to as high a temperature as measured¹⁰³, even when the inferred l would be smaller than λ , which would violate the Heisenberg uncertainty principle for the quasiparticles. Moreover, the Hall resistivity has a temperature dependence different from what would be expected in a quasiparticle picture¹⁰⁴.

In the late 1980s, some of these and various other experimental anomalies were encapsulated in the phenomenological ‘marginal Fermi liquid’ theory⁵. This asserts that the Fermi gas is coupled to a continuum of excitations that is spatially featureless, with a spectral density which is constant for $\omega > T$, but proportional to T for $\omega < T$. This leads to a damping rate that scales as $\max(\omega, T)$. This was confirmed later by high-resolution ARPES measurements, with the caveat that this is only seen in the nodal region, with the antinodal region behaving in a more incoherent fashion¹⁰⁵.

In the 1990s it was proposed that quantum criticality could explain the low-energy excitations of the strange metal. A quantum phase transition occurs when a continuous phase transition occurs at zero temperature as a function of a tuning parameter (like pressure or doping), where the corresponding QCP defines the boundary between the ordered (broken symmetry) and disordered quantum phases¹⁰⁶. The correlations at a QCP are characterized by a spatio-temporal scale invariance, which in turn has the effect that there are no longer quasiparticle poles (δ -functions) in spectral functions. Instead one finds power-law behaviour (‘branch cuts’) and spectral functions at finite temperature that are scaling functions of ω/T . This can be interpreted in terms of a dissipative energy relaxation time $\hbar/k_B T$, which is sometimes referred to as “Planckian dissipation” because it is a quantum effect independent of material parameters¹⁰⁷. Moving away from the critical point, the energy scale above which scale invariance remains gradually increases. Accordingly, in the ‘tuning parameter’–temperature plane, there is a quantum critical wedge opening up from the QCP. This suggests an interpretation of the phase diagram in Fig. 2, where the strange metal is identified with the quantum critical wedge associated with a QCP under the superconducting dome near optimal doping.

The theory of quantum criticality in metallic systems is still a work in progress. One issue is that there may be reasons to believe that the QCP is intrinsically unstable, since the order parameter fluctuations mediate attractive interactions that promote superconductivity, meaning that the QCP might always be ‘shielded’ by a superconducting dome, just as in Fig. 2. However, there is also typically a diverging correlation length at a QCP, while no such growing correlation length has yet been observed in the strange metal state of the copper oxides for any of the orders that are considered likely candidates. Moreover, according to the marginal Fermi liquid phenomenology⁵, what is needed is a special sort of quantum criticality that is local in space, and so featureless in k .

Is there a QCP involving the termination of pseudogap order inside the superconducting dome? There is evidence for the termination of pseudogap order in a QCP from early specific heat data¹⁰⁸ and from a dispersion anomaly seen in photoemission¹⁰⁹ as well as a vanishing of the Kerr rotation¹⁰² and charge order⁹², with the latest being a divergence in the effective mass seen in quantum oscillation studies¹¹⁰. But which order parameter rules the quantum critical regime¹¹¹, and is that regime large enough to encompass the entire strange metal region? We argued above that the pseudogap is characterized by several competing ordering tendencies. Even more seriously, this quantum critical description should break down at higher temperatures. But the strange metal persists to the highest attainable temperatures.

For a highly correlated fluid, the interactions are large and so probably cannot be treated using any fundamentally perturbative approach which starts with a free particle description. There is a well-developed and extremely successful theoretical solution of this problem applicable to one-dimensional and quasi-one-dimensional electron fluids based on ‘bosonization’, but no such approach exists in higher dimensions. In this context, it is important to seek new approaches— theories that honestly treat the strong correlation physics—even if the connection to the relevant microscopic physics is unclear. This is where the mathematics of string

theory may help: with the so-called holographic duality, one can address the physics of strongly interacting finite density systems. Its central point, the mathematical anti-deSitter to conformal field theory (AdS/CFT) correspondence, has become a focus for modern string theoretical research. Discovered in 1997¹¹², it demonstrates that the two grand theories of physics, which seem unrelated (general relativity and quantum field theory) can become under certain conditions two sides of the same coin. According to the correspondence, there is a ‘holographic’ relation in the sense that the quantum field theory is like a two-dimensional photographic plate with interference fringes encoding the gravitational physics in three dimensions. Most importantly, the difficult-to-solve strong-coupling quantum field theory is mapped to its more easily solved holographic dual, the weak-coupling gravity theory.

Since 2007, the properties of matter at finite density have been the central focus of this ‘holography’ research¹¹³. At low temperatures one finds superconductors, stripe and current phases, and even Fermi liquids. The observable responses of these states are often similar to experimental observations. However, the great difference is in the nature of the strange metal at higher temperatures. The gravity dual tells us that these systems at finite fermion density should form metallic quantum critical phases, where the scale invariance emerges without fine tuning to any special QCP. However, these ‘conformal’ metals (which exhibit Planckian dissipation) are intrinsically unstable, and upon cooling spawn an extensive manifold of stable states. They also have special scaling properties that are different from any conventional quantum critical state¹¹⁴.

Owing to the limitations of the mathematics, holography can only be proved for certain field theories that have no resemblance whatsoever with the electrons in the copper oxides. It is not currently known whether the traits discussed above are ubiquitous emergent phenomena or somehow tied to these special cases. At the least, however, holography may supply powerful new metaphors, teaching physicists to think differently, and leading to new experimental questions.

The overdoped regime

As the doping is increased beyond the doping optimal for the superconductivity, it appears that a real Fermi liquid begins to be established: quantum oscillations indicate a well-developed large Fermi surface, consistent in detail with the prediction of one electron band theory¹¹⁵. This is supported by ARPES measurements where now sharp peaks are observed near this Fermi surface throughout the Brillouin zone (including the antinodes)^{45,116}. Inelastic neutron scattering data indicate a dramatic suppression of magnetic spectral weight near the antiferromagnetic wave vectors, which may be interpreted as a disappearance of the spin-fluctuation pairing glue, explaining why T_c goes down¹¹⁷. On the other hand, recent resonant inelastic X-ray scattering data have demonstrated pronounced spin fluctuations at smaller wave vectors, implying that strong electron correlations persist even in highly overdoped copper oxides^{33,118}. A big question is how different the Fermi liquid at lower temperatures really is from the anomalous strange metal at higher temperatures. ARPES shows that there is only a weak crossover line that separates these two regimes¹¹⁹.

Outlook

Originally inspired by the desire to find out why superconductivity can happen at a high temperature, condensed matter scientists engaged in a relentless effort to unravel the physics of copper oxides. As we have emphasized, there is still plenty of work to do, especially with regards to the physics of competing order in the underdoped regime. The bottom line is that the existing theoretical machinery seems inadequate to describe both the rich physics of the pseudogap phase and the nature of the strange metal phase.

Experimental techniques with which to control correlated electrons are evolving rapidly. Recent examples include the development of atomically precise layer-deposition methods that allow the tailoring of lattice structures¹²⁰ and coherent optical control techniques⁷⁴. In another development, the practitioners of quantum information and string theory have landed in the same territory, finding to their surprise that they are struggling with

many of the same issues as condensed matter physicists. This is also reflected in the fact that some of the key underlying physics has been captured by advanced numerical techniques like the density matrix renormalization group and its descendants²⁹, which were also motivated by quantum information theory. The jury is still out on whether this is a coincidence or signals the onset of a revolution in physics.

Received 28 October; accepted 22 December 2014.

1. Bednorz, J. G. & Müller, K. A. Possible high T_c superconductivity in the Ba-La-Cu-O system. *Z. Phys. B* **64**, 189–193 (1986).
2. Bardeen, J., Cooper, L. N. & Schrieffer, J. R. Theory of superconductivity. *Phys. Rev.* **108**, 1175–1204 (1957).
3. Cohen, M. & Anderson, P. W. Comments on the maximum superconducting transition temperature. In *Superconductivity in d- and f-band Metals* (ed. Douglas, D. H.) 17–27 (American Institute of Physics, 1972).
4. Nagamatsu, J., Nakagawa, N., Muranaka, T., Zenitani, Y. & Akimitsu, J. Superconductivity at 39 K in magnesium diboride. *Nature* **410**, 63–64 (2001).
5. Varma, C. M., Littlewood, P. B., Schmitt-Rink, S., Abrahams, E. & Ruckenstein, A. E. Phenomenology of the normal state of Cu-O high-temperature superconductors. *Phys. Rev. Lett.* **63**, 1996–1999 (1989).
6. Hussey, N. E., Takenaka, K. & Takagi, H. Universality of the Mott-Ioffe-Regel limit of metals. *Phil. Mag.* **84**, 2847–2864 (2004).
7. Fradkin, E., Kivelson, S. A. & Tranquada, J. M. Theory of intertwined orders in high-temperature superconductors. Preprint at <http://arXiv.org/abs/1407.4480> (2014).
8. Wollman, D. A., Van Harlingen, D. J., Lee, W. C., Ginsberg, D. M. & Leggett, A. J. Experimental determination of the superconducting pairing state in YBCO from the phase coherence of YBCO-Pb dc SQUIDs. *Phys. Rev. Lett.* **71**, 2134–2137 (1993).
9. Tsuei, C. C. & Kirtley, J. R. Pairing symmetry in cuprate superconductors. *Rev. Mod. Phys.* **72**, 969–1016 (2000).
10. Scalapino, D. J., Loh, E. & Hirsch, J. E. d-wave pairing near a spin-density-wave instability. *Phys. Rev. B* **34**, 8190–8192 (1986).
11. Miyake, K., Schmitt-Rink, S. & Varma, C. M. Spin-fluctuation-mediated even-parity pairing in heavy-fermion superconductors. *Phys. Rev. B* **34**, 6554–6556 (1986).
12. Béal-Monod, M. T., Bourbonnais, C. & Emery, V. J. Possible superconductivity in nearly antiferromagnetic itinerant fermion systems. *Phys. Rev. B* **34**, 7716–7720 (1986).
13. Dahm, T. et al. Strength of the spin-fluctuation-mediated pairing interaction in a high-temperature superconductor. *Nature Phys.* **5**, 217–221 (2009).
14. Zaanen, J. Watching rush hour in the world of electrons. *Science* **315**, 1372–1373 (2007).
15. Anderson, P. W. The resonating valence bond state in La_2CuO_4 and superconductivity. *Science* **235**, 1196–1198 (1987).
16. Vaknin, D. et al. Antiferromagnetism in $\text{La}_2\text{CuO}_{4-y}$. *Phys. Rev. Lett.* **58**, 2802–2805 (1987).
17. Chakravarty, S., Halperin, B. I. & Nelson, D. R. Low-temperature behavior of two-dimensional quantum antiferromagnets. *Phys. Rev. Lett.* **60**, 1057–1060 (1988).
18. Doiron-Leyraud, N. et al. Quantum oscillations and the Fermi surface in an underdoped high- T_c superconductor. *Nature* **447**, 565–568 (2007).
- First quantum oscillation evidence for a distinct electronic state with a reconstructed Fermi surface, realized in the underdoped copper oxides under intense magnetic fields.**
19. Sebastian, S. E. et al. Normal-state nodal electronic structure in underdoped high- T_c copper oxides. *Nature* **511**, 61–64 (2014).
20. Zaanen, J. & Gunnarsson, O. Charged magnetic domain lines and the magnetism of high- T_c oxides. *Phys. Rev. B* **40**, 7391–7394 (1989).
21. Emery, V. J. & Kivelson, S. A. Frustrated electronic phase separation and high-temperature superconductors. *Physica C* **209**, 597–621 (1993).
22. Tranquada, J. M., Sternlieb, B. J., Axe, J. D., Nakamura, Y. & Uchida, S. Evidence for stripe correlations of spins and holes in copper oxide superconductors. *Nature* **375**, 561–563 (1995).
- First evidence from neutron scattering for modulated spin and charge order in underdoped copper oxides.**
23. Raghu, S., Kivelson, S. A. & Scalapino, D. J. Superconductivity in the repulsive Hubbard model: an asymptotically exact weak-coupling solution. *Phys. Rev. B* **81**, 224505 (2010).
24. Scalapino, D. J. A common thread: the pairing interaction for unconventional superconductors. *Rev. Mod. Phys.* **84**, 1383–1417 (2012).
- A comprehensive review of spin fluctuation pairing theories for superconductivity.**
25. Liu, L., Yao, H., Berg, E., White, S. R. & Kivelson, S. A. Phases of the infinite U Hubbard model on square lattices. *Phys. Rev. Lett.* **108**, 126406 (2012).
26. Lee, P. A., Nagaosa, N. & Wen, X.-G. Doping a Mott insulator: physics of high-temperature superconductivity. *Rev. Mod. Phys.* **78**, 17–85 (2006).
- An overview of strong coupling models of copper oxides from the doped Mott insulator view, focusing on the resonating valence bond picture.**
27. Parameshwari, A., Randeria, M. & Trivedi, N. High- T_c superconductors: a variational theory of the superconducting state. *Phys. Rev. B* **70**, 054504 (2004).
28. Georges, A., Kotliar, G., Krauth, W. & Rozenberg, M. J. Dynamical mean-field theory of strongly correlated fermion systems and the limit of infinite dimensions. *Rev. Mod. Phys.* **68**, 13–125 (1996).
- Fundamentals of dynamical mean field theory are discussed in this authoritative review.**
29. Stoudenmire, E. M. & White, S. R. Studying two-dimensional systems with the density matrix renormalization group. *Annu. Rev. Condens. Matter Phys.* **3**, 6.1–6.18 (2012).
- An introduction to density matrix renormalization group studies of two-dimensional materials, including tensor network generalizations.**
30. White, S. R. & Scalapino, D. J. Density matrix renormalization group study of the striped phase in the 2D t-J model. *Phys. Rev. Lett.* **80**, 1272–1275 (1998).
31. Corboz, P., Rice, T. M. & Troyer, M. Competing states in the t-J model: uniform d-wave state versus stripe state. *Phys. Rev. Lett.* **113**, 046402 (2014).
32. Le Tacon, M. et al. Intense paramagnon excitations in a large family of high-temperature superconductors. *Nature Phys.* **7**, 725–730 (2011).
33. Dean, M. P. M. et al. Persistence of magnetic excitations in $\text{La}_{2-x}\text{Sr}_x\text{CuO}_4$ from the undoped insulator to the heavily overdoped non-superconducting metal. *Nature Mater.* **12**, 1019–1023 (2013).
34. Fong, H. F. et al. Spin susceptibility in underdoped $\text{YBa}_2\text{Cu}_3\text{O}_{6+x}$. *Phys. Rev. B* **61**, 14773–14786 (2000).
35. Dai, P., Mook, H. A., Hunt, R. D. & Dogan, F. Evolution of the resonance and incommensurate spin fluctuations in superconducting $\text{YBa}_2\text{Cu}_3\text{O}_{6+x}$. *Phys. Rev. B* **63**, 054525 (2001).
36. Carbotte, J. P., Timusk, T. & Hwang, J. Bosons in high-temperature superconductors: an experimental survey. *Rep. Prog. Phys.* **74**, 066501 (2011).
37. Anderson, P. W. Is there glue in cuprate superconductors? *Science* **316**, 1705–1707 (2007).
38. Lanzara, A. et al. Evidence for ubiquitous strong electron-phonon coupling in high-temperature superconductors. *Nature* **412**, 510–514 (2001).
39. Reznik, D. et al. Electron-phonon coupling reflecting dynamic charge inhomogeneity in copper oxide superconductors. *Nature* **440**, 1170–1173 (2006).
40. Leggett, A. J. A “midinfrared” scenario for cuprate superconductivity. *Proc. Natl Acad. Sci. USA* **96**, 8365–8372 (1999).
41. Abrinkov, A. A. & Gor'kov, L. P. Contribution to the theory of superconducting alloys with paramagnetic impurities. *Sov. Phys. JETP* **12**, 1243–1253 (1961).
42. Garg, A., Randeria, M. & Trivedi, N. Strong correlations make high-temperature superconductors robust against disorder. *Nature Phys.* **4**, 762–765 (2008).
43. Uemura, Y. J. et al. Universal correlations between T_c and n_e/m^* in high- T_c cuprate superconductors. *Phys. Rev. Lett.* **62**, 2317–2320 (1989).
44. Emery, V. J. & Kivelson, S. A. Importance of phase fluctuations in superconductors with small superfluid density. *Nature* **374**, 434–437 (1995).
45. Chatterjee, U. et al. Electronic phase diagram of high-temperature copper oxide superconductors. *Proc. Natl Acad. Sci. USA* **108**, 9346–9349 (2011).
46. Matsui, H. et al. BCS-like Bogoliubov quasiparticles in high- T_c superconductors observed by angle-resolved photoemission spectroscopy. *Phys. Rev. Lett.* **90**, 217002 (2003).
47. Fedorov, A. V. et al. Temperature dependent photoemission studies of optimally doped $\text{Bi}_2\text{Sr}_2\text{Ca}_2\text{O}_8$. *Phys. Rev. Lett.* **82**, 2179–2182 (1999).
48. Feng, D. L. et al. Signature of superfluid density in the single-particle excitation spectrum of $\text{Bi}_2\text{Sr}_2\text{Ca}_2\text{O}_{8+\delta}$. *Science* **289**, 277–281 (2000).
49. Warren, W. W. et al. Cu spin dynamics and superconducting precursor effects in planes above T_c in $\text{YBa}_2\text{Cu}_3\text{O}_{6.7}$. *Phys. Rev. Lett.* **62**, 1193–1196 (1989).
50. Alloul, H., Ohno, T. & Mendels, P. ^{89}Y NMR evidence for a Fermi-liquid behavior in $\text{YBa}_2\text{Cu}_3\text{O}_{6+x}$. *Phys. Rev. Lett.* **63**, 1700–1703 (1989).
51. Homes, C. C., Timusk, T., Liang, R., Bonn, D. A. & Hardy, W. N. Optical conductivity of c axis oriented $\text{YBa}_2\text{Cu}_3\text{O}_{6.70}$: evidence for a pseudogap. *Phys. Rev. Lett.* **71**, 1645–1648 (1993).
52. Puchkov, A. V., Basov, D. N. & Timusk, T. The pseudogap state in high- T_c superconductors: an infrared study. *J. Phys. Condens. Matter* **8**, 10049–10082 (1996).
53. Bucher, B., Steiner, P., Karpinski, J., Kaldus, E. & Wachter, P. Influence of the spin gap on the normal state transport in $\text{YBa}_2\text{Cu}_4\text{O}_8$. *Phys. Rev. Lett.* **70**, 2012–2015 (1993).
54. Ito, T., Takenaka, K. & Uchida, S. Systematic deviation from T-linear behavior in the in-plane resistivity of $\text{YBa}_2\text{Cu}_3\text{O}_{7-y}$: evidence for dominant spin scattering. *Phys. Rev. Lett.* **70**, 3995–3998 (1993).
55. Hashimoto, M. et al. Energy gaps in high-transition-temperature cuprate superconductors. *Nature Phys.* **10**, 483–495 (2014).
56. Norman, M. R. et al. Destruction of the Fermi surface in underdoped high- T_c superconductors. *Nature* **392**, 157–160 (1998).
57. Marshall, D. S. et al. Unconventional electronic structure evolution with hole doping in $\text{Bi}_2\text{Sr}_2\text{CaCu}_2\text{O}_{8+\delta}$: angle-resolved photoemission results. *Phys. Rev. Lett.* **76**, 4841–4844 (1996).
- First indication from photoemission of a pseudogap and reconstructed Fermi surface in underdoped copper oxides.**
58. Yang, H.-B. et al. Emergence of preformed Cooper pairs from the doped Mott insulating state in $\text{Bi}_2\text{Sr}_2\text{CaCu}_2\text{O}_{8+\delta}$. *Nature* **456**, 77–80 (2008).
59. Hoffman, J. E. et al. Imaging quasiparticle interference in $\text{Bi}_2\text{Sr}_2\text{CaCu}_2\text{O}_{8+\delta}$. *Science* **297**, 1148–1151 (2002).
- First study of quasiparticle interference in copper oxides obtained from a Fourier transform of scanning tunnelling spectra.**
60. McElroy, K. et al. Relating atomic-scale electronic phenomena to wave-like quasiparticle states in superconducting $\text{Bi}_2\text{Sr}_2\text{CaCu}_2\text{O}_{8+\delta}$. *Nature* **422**, 592–596 (2003).
61. Kohsaka, Y. et al. How Cooper pairs vanish approaching the Mott insulator in $\text{Bi}_2\text{Sr}_2\text{CaCu}_2\text{O}_{8+\delta}$. *Nature* **454**, 1072–1078 (2008).
62. Fujita, K. et al. Simultaneous transitions in cuprate momentum-space topology and electronic symmetry breaking. *Science* **344**, 612–616 (2014).

63. Vishik, I. M. *et al.* A momentum-dependent perspective on quasiparticle interference in $\text{Bi}_2\text{Sr}_2\text{CaCu}_2\text{O}_{8+\delta}$. *Nature Phys.* **5**, 718–721 (2009).
64. Vershinin, M. *et al.* Local ordering in the pseudogap state of the high- T_c superconductor $\text{Bi}_2\text{Sr}_2\text{CaCu}_2\text{O}_{8+\delta}$. *Science* **303**, 1995–1998 (2004).
65. Parker, C. V. *et al.* Fluctuating stripes at the onset of the pseudogap in the high- T_c superconductor $\text{Bi}_2\text{Sr}_2\text{CaCu}_2\text{O}_{8+x}$. *Nature* **468**, 677–680 (2010).
66. Howald, C., Eisaki, H., Kaneko, N. & Kapitulnik, A. Coexistence of periodic modulation of quasiparticle states and superconductivity in $\text{Bi}_2\text{Sr}_2\text{CaCu}_2\text{O}_{8+\delta}$. *Proc. Natl Acad. Sci. USA* **100**, 9705–9709 (2003).
67. da Silva Neto, E. H. *et al.* Ubiquitous interplay between charge ordering and high-temperature superconductivity in cuprates. *Science* **343**, 393–396 (2014).
68. Comin, R. *et al.* Charge order driven by Fermi-arc instability in $\text{Bi}_{2-x}\text{La}_x\text{CuO}_{6+\delta}$. *Science* **343**, 390–392 (2014).
69. Ding, H. *et al.* Spectroscopic evidence for a pseudogap in the normal state of underdoped high- T_c superconductors. *Nature* **382**, 51–54 (1996).
70. Loeser, A. G. *et al.* Excitation gap in the normal state of underdoped $\text{Bi}_2\text{Sr}_2\text{CaCu}_2\text{O}_{8+\delta}$. *Science* **273**, 325–329 (1996).
71. Corson, J., Mallozzi, R., Orenstein, J., Eckstein, J. N. & Bozovic, I. Vanishing of phase coherence in underdoped $\text{Bi}_2\text{Sr}_2\text{CaCu}_2\text{O}_{8+\delta}$. *Nature* **398**, 221–223 (1999).
72. Li, L. *et al.* Diamagnetism and Cooper pairing above T_c in cuprates. *Phys. Rev. B* **81**, 054510 (2010).
73. Dubroka, A. *et al.* Evidence of a precursor superconducting phase at temperatures as high as 180 K in $\text{RBa}_2\text{Cu}_3\text{O}_{7-\delta}$ ($R = \text{Y}, \text{Gd}, \text{Eu}$) superconducting crystals from infrared spectroscopy. *Phys. Rev. Lett.* **106**, 047006 (2011).
74. Kaiser, S. *et al.* Optically induced coherent transport far above T_c in underdoped $\text{YBa}_2\text{Cu}_3\text{O}_{6+\delta}$. *Phys. Rev. B* **89**, 184516 (2014).
75. Norman, M. R. *et al.* Modeling the Fermi arc in underdoped cuprates. *Phys. Rev. B* **76**, 174501 (2007).
76. Reber, T. J. *et al.* The origin and non-quasiparticle nature of Fermi arcs in $\text{Bi}_2\text{Sr}_2\text{CaCu}_2\text{O}_{8+\delta}$. *Nature Phys.* **8**, 606–610 (2012).
77. Lee, J. *et al.* Spectroscopic fingerprint of phase-incoherent superconductivity in the underdoped $\text{Bi}_2\text{Sr}_2\text{CaCu}_2\text{O}_{8+\delta}$. *Science* **325**, 1099–1103 (2009).
78. Chakravarty, S., Laughlin, R. B., Morr, D. K. & Nayak, C. Hidden order in the cuprates. *Phys. Rev. B* **63**, 094503 (2001).
79. Scalapino, D. J. & White, S. R. Stripe structures in the t-t'-J model. *Physica C* **481**, 146–152 (2012).
80. Tajima, S., Noda, T., Eisaki, H. & Uchida, S. c-Axis optical response in the static stripe ordered phase of the cuprates. *Phys. Rev. Lett.* **86**, 500–503 (2001).
81. Li, Q., Hücker, M., Gu, G. D., Tsvelik, A. M. & Tranquada, J. M. Two-dimensional superconducting fluctuations in stripe-ordered $\text{La}_{1.875}\text{Ba}_{0.125}\text{CuO}_4$. *Phys. Rev. Lett.* **99**, 067001 (2007).
82. Arai, M. *et al.* Incommensurate spin dynamics of underdoped superconductor $\text{YBa}_2\text{Cu}_3\text{O}_{6.7}$. *Phys. Rev. Lett.* **83**, 608–611 (1999).
83. Ulbrich, H. & Braden, M. Neutron scattering studies on stripe phases in non-cuprate materials. *Physica C* **481**, 31–45 (2012).
84. Hinkov, V. *et al.* Spin dynamics in the pseudogap state of a high-temperature superconductor. *Nature Phys.* **3**, 780–785 (2007).
85. Norman, M. R. Linear response theory and the universal nature of the magnetic excitation spectrum of the cuprates. *Phys. Rev. B* **75**, 184514 (2007).
86. Wu, T. *et al.* Magnetic-field-induced charge-stripe order in the high-temperature superconductor $\text{YBa}_2\text{Cu}_3\text{O}_y$. *Nature* **477**, 191–194 (2011).
87. Tabis, W. *et al.* Connection between charge-density-wave order and charge transport in the cuprate superconductors. *Nature Commun.* **5**, 5875 (2014).
88. Ghiringhelli, G. *et al.* Long-range incommensurate charge fluctuations in $(\text{Y}, \text{Nd})\text{Ba}_2\text{Cu}_3\text{O}_{6+x}$. *Science* **337**, 821–825 (2012).
- Demonstration of charge crystallization without spin order as a generic ordering phenomenon in underdoped copper oxides, using resonant X-ray scattering.**
89. Chang, J. *et al.* Direct observation of competition between superconductivity and charge density wave order in $\text{YBa}_2\text{Cu}_3\text{O}_{6.67}$. *Nature Phys.* **8**, 871–876 (2012).
90. Le Tacon, M. *et al.* Inelastic X-ray scattering in $\text{YBa}_2\text{Cu}_3\text{O}_{6.6}$ reveals giant phonon anomalies and elastic central peak due to charge-density-wave formation. *Nature Phys.* **10**, 52–58 (2014).
91. Wu, T. *et al.* Short-range charge order reveals the role of disorder in the pseudogap state of high- T_c superconductors. Preprint at <http://arXiv.org/abs/1404.1617> (2014).
92. Blanco-Canosa, S. *et al.* Resonant X-ray scattering study of charge density wave correlations in $\text{YBa}_2\text{Cu}_3\text{O}_{6+x}$. *Phys. Rev. B* **90**, 054513 (2014).
93. Kivelson, S. A., Fradkin, E. & Emery, V. J. Electronic liquid-crystal phases of a doped Mott insulator. *Nature* **393**, 550–553 (1998).
94. Ando, Y., Segawa, K., Komiya, S. & Lavrov, A. N. Electrical resistivity anisotropy from self-organized one dimensionality in high-temperature superconductors. *Phys. Rev. Lett.* **88**, 137005 (2002).
95. Daou, R. *et al.* Broken rotational symmetry in the pseudogap phase of a high- T_c superconductor. *Nature* **463**, 519–522 (2010).
96. Hinkov, V. *et al.* Electronic liquid crystal state in the high-temperature superconductor $\text{YBa}_2\text{Cu}_3\text{O}_{6.45}$. *Science* **319**, 597–600 (2008).
97. Kivelson, S. A. *et al.* How to detect fluctuating stripes in the high-temperature superconductors. *Rev. Mod. Phys.* **75**, 1201–1241 (2003).
- A pedagogical treatise of electronic charge order and how to study it experimentally.**
98. Lawler, M. J. *et al.* Intra-unit-cell electronic nematicity of the high- T_c copper-oxide pseudogap states. *Nature* **466**, 347–351 (2010).
99. da Silva Neto, E. H. *et al.* Detection of electronic nematicity using scanning tunneling microscopy. *Phys. Rev. B* **87**, 161117 (2013).
100. Fauqué, B. *et al.* Magnetic order in the pseudogap phase of high- T_c superconductors. *Phys. Rev. Lett.* **96**, 197001 (2006).
101. Varma, C. M. Non-Fermi-liquid states and pairing instability of a general model of copper oxide metals. *Phys. Rev. B* **55**, 14554–14580 (1997).
102. Xia, J. *et al.* Polar Kerr-effect measurements of the high-temperature $\text{YBa}_2\text{Cu}_3\text{O}_{6+x}$ superconductor: evidence for broken symmetry near the pseudogap temperature. *Phys. Rev. Lett.* **100**, 127002 (2008).
103. Martin, S., Fiory, A. T., Fleming, R. M., Schneemeyer, L. F. & Waszczak, J. V. Normal-state transport properties of $\text{Bi}_{2+x}\text{Sr}_{2-y}\text{CuO}_{6+\delta}$ crystals. *Phys. Rev. B* **41**, 846–849 (1990).
104. Chien, T. R., Wang, Z. Z. & Ong, N. P. Effect of Zn impurities on the normal-state Hall angle in single-crystal $\text{YBa}_2\text{Cu}_{3-x}\text{Zn}_x\text{O}_{7-\delta}$. *Phys. Rev. Lett.* **67**, 2088–2091 (1991).
105. Valla, T. *et al.* Temperature dependent scattering rates at the Fermi surface of optimally doped $\text{Bi}_2\text{Sr}_2\text{CaCu}_2\text{O}_{8+\delta}$. *Phys. Rev. Lett.* **85**, 828–831 (2000).
106. Sachdev, S. *Quantum Phase Transitions* (Cambridge Univ. Press, 1999).
- An authoritative text covering the fundamentals of quantum phase transitions.**
107. Zaanen, J. Superconductivity: why the temperature is high. *Nature* **430**, 512–513 (2004).
108. Tallon, J. L., Williams, G. V. M., Staines, M. P. & Bernhard, C. Energy and length scales in the superconducting phase diagram for HTSC cuprates. *Physica C* **235–240**, 1821–1822 (1994).
109. Vishik, I. M. *et al.* Phase competition in trisection superconducting dome. *Proc. Natl Acad. Sci. USA* **109**, 18332–18337 (2012).
110. Ramshaw, B. J. *et al.* A quantum critical point at the heart of high temperature superconductivity. Preprint at <http://arXiv.org/abs/1409.3990> (2014).
111. Castellani, C., Di Castro, C. & Grilli, M. Singular quasiparticle scattering in the proximity of charge instabilities. *Phys. Rev. Lett.* **75**, 4650–4653 (1995).
112. Maldacena, J. M. The large N limit of superconformal field theories and supergravity. *Adv. Theor. Math. Phys.* **2**, 231–252 (1998).
113. Zaanen, J., Sun, Y. W., Liu, Y. & Schalm, K. *Holographic Duality for Condensed Matter Physics* (Cambridge Univ. Press, in the press).
- A comprehensive but accessible text for condensed matter applications of the AdS/CFT correspondence.**
114. Iqbal, N., Liu, H. & Mezei, M. Lectures on holographic non-Fermi liquids and quantum phase transitions. In *String Theory and Its Applications, TASI 2010*, (eds Dine, M., Banks, T. & Sachdev, S.) 707–816 (World Scientific, 2012).
115. Vignolle, D. *et al.* Quantum oscillations in an overdoped high- T_c superconductor. *Nature* **455**, 952–955 (2008).
116. Platé, M. *et al.* Fermi surface and quasiparticle excitations of overdoped $\text{Tl}_2\text{Ba}_2\text{CuO}_{6+\delta}$. *Phys. Rev. Lett.* **95**, 077001 (2005).
117. Wakimoto, S. *et al.* Direct relation between the low-energy spin excitations and superconductivity of overdoped high- T_c superconductors. *Phys. Rev. Lett.* **92**, 217004 (2004).
118. Le Tacon, M. *et al.* Dispersive spin excitations in highly overdoped cuprates revealed by resonant inelastic x-ray scattering. *Phys. Rev. B* **88**, 020501 (2013).
119. Kaminski, A. *et al.* Crossover from coherent to incoherent electronic excitations in the normal state of $\text{Bi}_2\text{Sr}_2\text{CaCu}_2\text{O}_{8+\delta}$. *Phys. Rev. Lett.* **90**, 207003 (2003).
120. Gozar, A. *et al.* High-temperature interface superconductivity between metallic and insulating copper oxides. *Nature* **455**, 782–785 (2008).

Acknowledgements We thank A. Yazdani for many discussions. S.A.K. was supported by the US DOE, Basic Energy Sciences, Materials Science and Engineering, under Award No. DE-AC02-76SF00515 at Stanford University. M.N. was supported by the Center for Emergent Superconductivity, an Energy Frontier Research Center funded by the US DOE, Basic Energy Sciences, under Award No. DE-AC0298CH1088. J.Z. acknowledges financial support by the Netherlands Organization for Scientific Research/Ministry of Science and Education (NWO/OCW), and a grant from the Templeton foundation: the opinions expressed in this publication are those of the authors and do not necessarily reflect the views of the John Templeton foundation.

Author Contributions All authors contributed to the text. S.U. prepared the figures.

Author Information Reprints and permissions information is available at www.nature.com/reprints. The authors declare no competing financial interests. Readers are welcome to comment on the online version of the paper. Correspondence and requests for materials should be addressed to J.Z. (jan@lorentz.leidenuniv.nl).